



Antimicrobial and antifouling properties of versatile PPSU/carboxylated GO nanocomposite membrane against Gram-positive and Gram-negative bacteria and protein

Arun Kumar Shukla¹ · Javed Alam¹  · Mohammad Azam Ansari² · Mansour Alhoshan^{1,3} · Fekri Abdulraqueb Ahmed Ali³

Received: 19 March 2018 / Accepted: 12 September 2018 / Published online: 3 October 2018
© Springer-Verlag GmbH Germany, part of Springer Nature 2018

Abstract

Biofouling is a serious issue in membrane-based water and wastewater treatment as it critically compromises the efficacy of the water treatment processes. This investigation demonstrates the antimicrobial and antifouling properties of a nanocomposite membrane system composed of carboxyl-functionalized graphene oxide (COOH-GO) and polyphenylsulfone (PPSU). The PPSU/COOH-GO nanocomposite membrane exhibited excellent antimicrobial properties, achieving maximum bacteriostasis rates of 74.2% and 81.1% against the representative Gram-negative bacteria (*Escherichia coli* and *Pseudomonas aeruginosa*, respectively) and 41.9% against the representative Gram-positive bacterium (*Staphylococcus aureus*). The PPSU/COOH-GO nanocomposite membrane inhibited the attachment, colonization, and the biofilm formation of three species. Antifouling was assessed through filtration experiments using a model foulant bovine serum albumin (BSA). The fouling mechanisms were investigated by Hermia's models (complete blocking, intermediate blocking, standard blocking, and cake formation), and the analysis involved fitting the volumetric flux decline experimental data to models. The fouling study revealed a less irreversible fouling and increased flux recovery ratio for the PPSU/COOH-GO nanocomposite membrane. Complete blocking of pores and cake formation were the major fouling mechanisms for the membrane.

Keywords Carboxyl-functionalized graphene oxide · Antimicrobial · Antifouling · Nanocomposite membrane

Introduction

Membrane technology is a green, energy-efficient, and cost-efficient separation and purification technology with diverse potential applications in food processing, protein separation, biotechnology, pharmaceutical manufacture, reduction of mi-

croorganisms, and wastewater treatments (Shannon et al. 2008; Bogdanović et al. 2015; Lee et al. 2016; Koh and Lee 2017; Morelos-Gomez et al. 2017; Xu et al. 2017). However, practical application of membrane technology is hampered by membrane fouling, which reduces membrane performance stability and water flux, shortens the service life, and increases the maintenance and operational costs. Fouling is generally initiated by the growth and deposition of the foulants on membrane surface. Foulants include contaminating microorganisms, inorganic or organic compounds, and colloids (Wang and Tang 2011; Hu et al. 2016; Perreault et al. 2016; Emadzadeh et al. 2017; Hou et al. 2017; Ma et al. 2017; Shokravi et al. 2017; You et al. 2017; Corbatón-Báguena et al. 2018; Zhang et al. 2018b). Biofouling associated with microorganisms of microbial proteins is common and can lead to a biofilm formation on the surface of membranes. Biofilms result from the attachment and proliferation of bacteria. This colonization, along with the accumulation of secreted extracellular polysaccharides and proteins, can block the membrane pores, degrade the membrane, and reduce membrane

Responsible editor: Giovanni Benelli

✉ Javed Alam
javaalam@ksu.edu.sa

- ¹ King Abdullah Institute for Nanotechnology, King Saud University, P.O. Box 2455, Riyadh 11451, Kingdom of Saudi Arabia
- ² Department of Epidemic Disease Research, Institute of Research and Medical Consultation, Imam Abdulrahman Bin Faisal university, Dammam, Kingdom of Saudi Arabia
- ³ Chemical Engineering Department, College of Engineering, King Saud University, P.O. Box 800, Riyadh 11421, Kingdom of Saudi Arabia

flux (Ahmed et al. 2012; Perreault et al. 2016; Gao et al. 2017a; Hou et al. 2017; Liu et al. 2017; Srinivasan et al. 2018).

Elimination of membrane biofouling is challenging, since even low residual numbers of microorganisms can regenerate the biofilm. The ideal approach is to restrict the attachment and surface proliferation of Gram-positive bacteria and Gram-negative bacteria, with the goals of reducing the decomposition of essential metabolites, preserving cell membrane structure, and maintaining the activity of enzymes used for protein denaturation (Yu et al. 2013a; Koh and Lee 2017; Qiu et al. 2017; Zhang et al. 2018a). Membrane hydrophilicity, surface charge, and surface roughness also influence membrane fouling, and recent research efforts have focused on enhancing membrane surface hydrophilicity and charge through membrane modification (Yu et al. 2013a; Ben-Sasson et al. 2014; Emadzadeh et al. 2017; Zhu et al. 2017; Hu et al. 2018; Shukla et al. 2018). The numerous modification methods that have been applied include coating, grafting, and, germane to this study, mixed matrix membranes (Ho et al. 2017; Abdel-Karim et al. 2018; Moradi et al. 2018; Nasrollahi et al. 2018). Mixed matrix membranes can incorporate inorganic nanoparticles including carbon nanotubes, zinc oxide, titanium dioxide, aluminum oxide, silicon dioxide, nanogold, and graphene oxide (GO) (Safarpour et al. 2016; Chung et al. 2017; Shukla et al. 2017; Hu et al. 2018; Wang et al. 2018).

GO nanoparticles have been widely researched concerning membrane applications due to their superior physico-chemical properties caused by different functional groups, which render them bactericidal yet comparatively safe for humans (Akhavan and Ghaderi 2010; Benelli 2018). The carboxyl groups (COOH) on GO makes it easy to obtain hydrophilic and negatively charged membranes. GO forms strong complexes with water molecules, is outstandingly suited for membrane formation, and enhances antibacterial and antifouling properties of membranes (Luyts et al. 2013; Yu et al. 2015; Xu et al. 2016; Eng et al. 2017). GO also has reactive groups that can strongly interact with bacterial cells and easily cover cell surfaces. As a result, the surface affinity for bacteria is increased. GO has also been implicated as a possible antibiotic for bacteria because it can permanently damage bacteria by disrupting membrane potential (Gao et al. 2017b). The sharpened edges of GO can physically damage to bacterial walls. These collective advantages of GO may be useful in new antibacterial and antifouling technologies.

In pursuing our previous study on the nanocomposite membranes, comprising polyphenylsulfone (PPSU) and carboxylic-functionalized GO (COOH-GO), it was observed that carboxylated-GO produced a membrane with enhanced properties (such as surface charge, hydrophilicity and membrane morphology) that exhibited superior performance in terms of heavy metals removal. Here, we discuss the extraordinary potential of COOH-GO in developing a nanocomposite membrane with antimicrobial and antifouling properties.

The use of the COOH-GO nanofiller increased COOH capture through the formation of a strong complex with the PPSU matrix and produced an electrostatic interaction between negatively charged membrane and the foulants. The fabricated PPSU/COOH-GO nanocomposite membrane demonstrated the effective and long-lasting reduction of biofouling. The antibacterial performance of the membrane was examined using *Escherichia coli* and *Pseudomonas aeruginosa* as representative Gram-negative bacteria and *Staphylococcus aureus* as a representative Gram-positive species. The anti-fouling mechanisms were investigated using 1.0 g/l BSA as the model protein in the feed solutions using Hermia's models (complete blocking, intermediate blocking, standard blocking, and cake formation). The experimental data obtained during the ultrafiltration was compared with the predictions based on the cake formation, complete blocking of the membrane surfaces, and fouling mechanisms.

Materials and methods

Materials and chemicals

PPSU (Ultrason P 3010) was purchased from BASF (Germany). COOH-GO was supplied by Grafen Chemical Industries (Turkey). *N*-methyl-pyrrolidone (NMP; Loba Chemie, India) was used as a solvent. Polyethylene glycol (PEG, MW = 600), sodium lauryl sulfate, sodium azide, sodium chloride, disodium hydrogen phosphate dehydrate, and potassium dihydrogen phosphate were all purchased from Merck (Germany). BSA was procured from Sigma-Aldrich (USA). Deionized water prepared using the Milli-Q system (Millipore, USA) was consistently used.

Fabrication of membrane

A fabrication method of the resulting membranes was similar to our previously published paper (Shukla et al. 2018). According these methods, PPSU and PPSU/COOH-GO nanocomposite membranes were prepared through phase inversion technique. COOH-GO (0.5 wt%) was mixed to *N*-methyl-pyrrolidone solvent and sonicated for 1 h using a sonifier (Branson Ultrasonics Corporation, USA) to disperse the solvent and reduce aggregation. Vacuum-dried PPSU polymer (17.0 wt%) and polyethylene glycol additive (10 wt%) were then added to the solution mixture and stirred at 70 ± 5 °C for 24 h to produce a homogeneous solution. For membrane casting, the solution was poured onto a cleaned glass plate and spread out using a casting blade with a gap of 78 ± 3 μm and immersed into a non-solvent coagulation bath (water) at ambient temperature. Finally, the obtained membranes were washed a number of times using a distilled water and preserved in 0.2% sodium azide solution until further study.

Preparation of microbial suspension

The antimicrobial and antiadhesion properties of prepared membranes were determined using pure cultures of *E. coli* (ATCC-25922) and *P. aeruginosa* (ATCC-PAO1) as model Gram-negative bacteria and *S. aureus* (ATCC-9144) as the model Gram-positive bacterium. The bacteria were cultured in Nutrient Broth in a shaking incubator (200 rpm) at 37 °C for 24 h. The bacterial biomass of each culture was washed several times with phosphate buffered saline (PBS) to remove media. The final suspension of each culture was diluted in sterile 0.9% NaCl solution to a concentration of approximately 10^7 colony-forming units (CFU/ml).

Antimicrobial activity of membrane

The antimicrobial properties of the uncoated PPSU and PPSU/COOH-GO membranes were examined by standard plate count protocols to determine the viable number of each tested bacterium remaining in the suspensions. Bacteriostasis rates were used to quantitatively examine the antibacterial activities of PPSU/COOH-GO membranes. The PPSU and PPSU/COOH-GO membranes (6 cm²) were placed in 6-well flat bottom polystyrene plates (Sigma-Aldrich) containing 3×10^5 CFU/ml *E. coli*, *P. aeruginosa*, or *S. aureus* suspension for 6 h at 37 °C and 150 rpm. The membranes were removed from each bacterial suspension and were serially diluted 10-fold, with 100 µl of each diluted bacterial suspension spread onto agar plates and incubated for 24 h at 35 °C. The number of colonies that developed was analyzed using the standard plate count technique. The bacteriostasis rate (B_r) was calculated using Eq. (1):

$$B_r = (A - B/A) \times 100\% \quad (1)$$

where A is a number of the colonies of PPSU (control) membrane and B is a number of the colonies of PPSU/COOH-GO membrane.

Adhesion test

For adhesion testing, 6 cm² of each PPSU and PPSU/COOH-GO membrane was immersed in *E. coli*, *P. aeruginosa*, or *S. aureus* suspensions in 6-well flat bottom polystyrene plates (Sigma-Aldrich). The plates were incubated at 150 rpm and 37 °C for 6 h. Each membrane was removed and washed to eliminate planktonic bacteria and loosely attached bacteria. The membranes were fixed with 2.5% glutaraldehyde at 4 °C for 6 h; dehydration in a sequential series of 25, 50, 75, and 100% ethanol (10 min each); and dried at 30 °C in a desiccator. Samples were then mounted on stubs, coated with gold, and viewed using scanning electron microscopy (SEM) at an accelerating voltage of 20 kV (Ansari et al. 2014).

Antifouling properties of membrane

The volumetric flux of pure water (J_v) was measured at 2 bar TMP. BSA (1.0 g/l in 0.1 mol/l phosphate buffer, pH 7.0) as a model fouling protein was used as the feed solution at room temperature. The foulant volumetric flux (J_{vp}) data were collected at 15 min intervals during the filtration process using a filtration CF042 cell (Sterlitech, USA). An effective membrane area was approximately 42 cm². Subsequently, the fouled membrane samples were washed using deionized water and the final water volumetric flux (J_{v1}) was determined. The volumetric flux variation was used to evaluate the membrane fouling property, which was defined by the flux recovery ratio (J_vRR) using Eq. (2):

$$J_vRR (\%) = J_{v1}/J_v \times 100 \quad (2)$$

To study the fouling behavior of the membranes in further detail, several parameters including the total fouling ratio (R_t), reversible fouling ratio (R_r), and irreversible fouling ratio (R_{ir}) were defined using Eqs. (3)–(5), respectively (Huang et al. 2018):

$$R_t (\%) = (J_v - J_{vp})/J_v \times 100 \quad (3)$$

$$R_r (\%) = (J_{v1} - J_{vp})/J_v \times 100 \quad (4)$$

$$R_{ir} (\%) = (J_v - J_{v1})/J_v \times 100 \quad (5)$$

Statistical data analysis

The one-way analysis of variance (abbreviated one-way ANOVA) was used to determine the antimicrobial and antifouling properties of pure PPSU and PPSU/COOH-GO nanocomposite membranes whether there were any statistically significant differences between the means of two or more independent duration of interaction by against Gram-positive and Gram-negative bacteria and protein. ANOVA was performed with IBM SPSS® statistics software version 25. Tukey's HSD test was applied as post hoc test to compare the multiple treatments. All statistical data were checked for normality and equality of residual error variances assumptions of ANOVA.

Membrane fouling mechanism

To ascertain the potential mechanism of membrane fouling, Hermia proposed a mathematical model to define the declined volumetric flux during constant transmembrane pressure (TMP). The fouling mechanism was ascribed to four basic types of fouling: complete blocking, intermediate blocking, standard blocking, and cake formation models. These models are physically meaningful and therefore contribute to the understanding of the membrane fouling mechanisms. Hermia's

models can be written in a common mathematical equation shown in Eq. (6):

$$d^2t/dV^2 = K(dt/dV)^n \quad (6)$$

The fouling model was characterized by the value of n in Eq. (6). Complete blocking model ($n = 2$), standard blocking model ($n = 1.5$), intermediate pore blocking model ($n = 1$), and cake formation model ($n = 0$) are presented in Eq. (7)–(10), respectively (Ng et al. 2014):

$$\ln J_{vpt} = \ln J_{vp0} - K_c t \quad (7)$$

$$1/(J_{vpt})^{1/2} = 1/(J_{vp0})^{1/2} + K_S t \quad (8)$$

$$1/J_{vpt} = 1/J_{vp0} + K_i t \quad (9)$$

$$1/(J_{vpt})^2 = 1/(J_{vp0})^2 + K_{cf} t \quad (10)$$

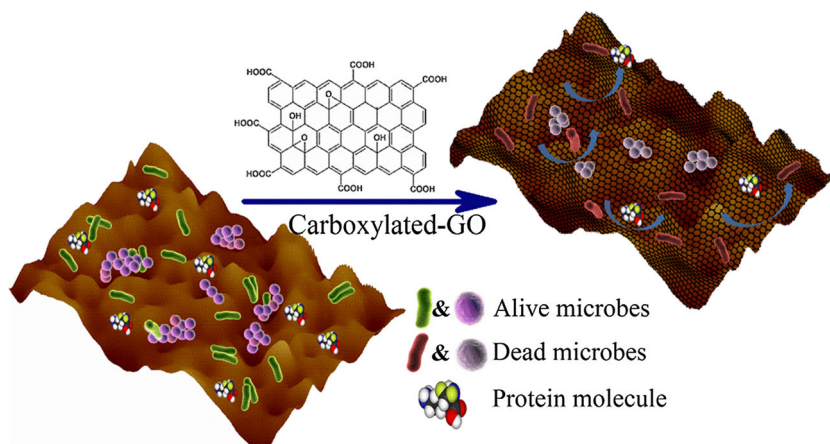
Results and discussion

Antimicrobial properties of membrane

The antimicrobial, antibiofilm, and antifouling properties of COOH-GO and polymeric membrane functionalized with graphene-based nanomaterials for Gram-negative and Gram-positive bacteria and biofilm forming microorganisms have been amply reported (Akhavan and Ghaderi 2010; Abinaya et al. 2018; Gurunathan et al. 2012; Yu et al. 2013b; Zhang et al. 2015; Ji et al. 2016; Gao et al. 2017b; Lu et al. 2017; Whitehead et al. 2017; Yousefi et al. 2017; Zou et al. 2017). However, the antimicrobial and antiadhesion activities of PPSU/COOH-GO have not been yet explored. The antimicrobial properties of pure PPSU and nanocomposite PPSU/COOH-GO membranes were presently assessed using *E. coli*, *P. aeruginosa*, and *S. aureus* cultures (Fig. 1). Each tested

culture (1×10^7 CFU/ml) was exposed to prepared membranes at 37 °C for 6 h. After spreading on agar plates overnight, the number of bacterial colonies was determined. Viable counts of *E. coli*, *P. aeruginosa*, and *S. aureus* were higher on PPSU membranes than on PPSU/COOH-GO nanocomposite membranes (Fig. 2a, c, e). Furthermore, the counts on the PPSU/COOH-GO membranes significantly decreased after 6 h (Fig. 2b, d, f). It has previously been observed that the deposition of COOH-GO on the PPSU surface restricted biofouling and inhibited bacterial growth. As shown in Fig. 2, the viable count from the PPSU/COOH-GO nanocomposite was significantly decreased compared to the membrane prepared of pure PPSU. The bacteriostasis rates of the nanocomposite PPSU/COOH-GO membrane for *E. coli* and *P. aeruginosa* were 74.2% and 81.1%, respectively (Fig. 3). These values were similar to that reported for GO-functionalized hyperbranched polyethylenimine (HPEI)/polyethersulfone (PES) membranes (74.8%) against *E. coli* (Yu et al. 2013b). The 41.9% bacteriostasis rate of the PPSU/COOH-GO nanocomposite membrane against *S. aureus* (Fig. 3) was similar to the previous report of 53.7% inactivation of *S. aureus* using GO-functionalized polyvinylidene fluoride membranes (Zeng et al. 2016). The values of F , df , and P were showed 115.253, 2, and 0.001 by using through the statistical analysis and post-hoc letters from ANOVA followed by Tukey's HSD test. The data clearly indicate that Gram-negative bacteria were affected more by COOH-GO than the Gram-positive species. This superior antimicrobial activity for *E. coli* and *P. aeruginosa* is likely attributed to the physical puncture of bacterial cells) and chemical effects, such as oxidative stress, that occur when the bacteria directly contact the PPSU/COOH-GO nanocomposite membrane (Gurunathan et al. 2012; Sanchez et al. 2012; Perreault et al. 2015). These findings implicate the PPSU/COOH-GO nanocomposite membrane as a promising nanomaterial for antifouling systems.

Fig. 1 Schematic model for antimicrobial and antifouling properties of nanocomposite membranes



Microbial adhesion

Polymeric membrane surfaces are readily colonized by bacteria that reside in the water that contacts the membrane. The bacteria can attach and proliferate to form biofilms. These biofilms represent a complex community of bacteria embedded in an extracellular polymeric matrix (Zodrow et al. 2009; Sawada et al. 2012). Biofilms develop on water filtration membrane units that are generally used in water treatment systems. This problem may be controlled if the adherence and colonization of bacteria on the membrane could be prevented. Prior studies have demonstrated that GO-functionalized membranes significantly restrict the attachment and biofilm formation of bacterial cells by disrupting the cell integrity and loss of cell viability (Akhavan and Ghaderi 2010; Hu et al. 2010; Mejías Carpio et al. 2012; Shanmuganathan et al. 2018).

In the present study, the attachment of both Gram-negative and Gram-positive bacteria on the surface of PPSU and PPSU/COOH-GO nanocomposite membranes was investigated

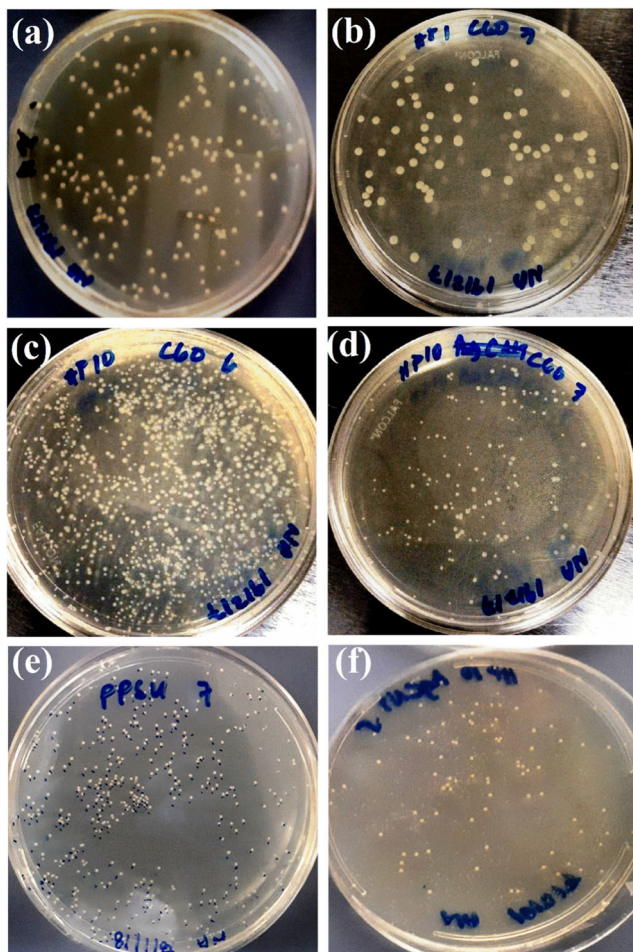


Fig. 2 Antimicrobial properties of membranes assessed by plate counting technique: **a** *E. coli*, **c** *P. aeruginosa*, and **e** *S. aureus* treated with PPSU (control) membrane; **b** *E. coli*, **d** *P. aeruginosa*, and **f** *S. aureus* treated with PPSU/COOH-GO nanocomposite membrane

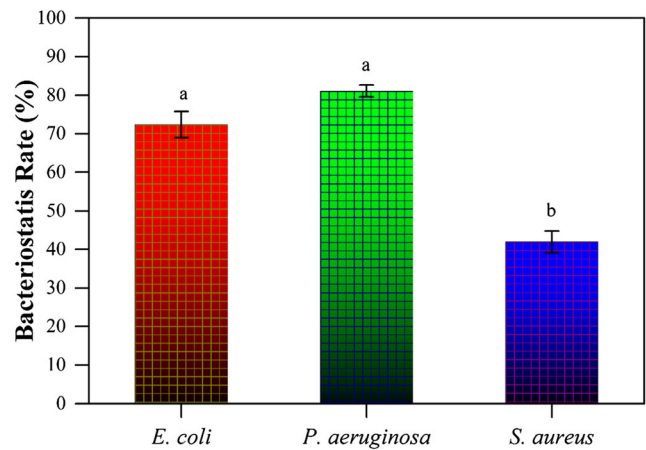


Fig. 3 Bacteriostasis rate (%) of PPSU/COOH-GO nanocomposite membrane against *E. coli*, *P. aeruginosa* and *S. aureus*. Different letters indicate significant differences ($p < 0.05$) between treatments using a one-way ANOVA with a post-hoc Tukey’s HSD test

using *E. coli*, *P. aeruginosa*, and *S. aureus*. After 12 h of incubation of the membranes with each of the bacterial cultures, bacteria that remained attached on the membrane surface were observed by SEM. Significant inhibition of biofilm formation and growth of all three bacteria were evident on PPSU/COOH-GO nanocomposite membranes (Fig. 4). In contrast, the biofilm formed by *E. coli*, *P. aeruginosa*, and

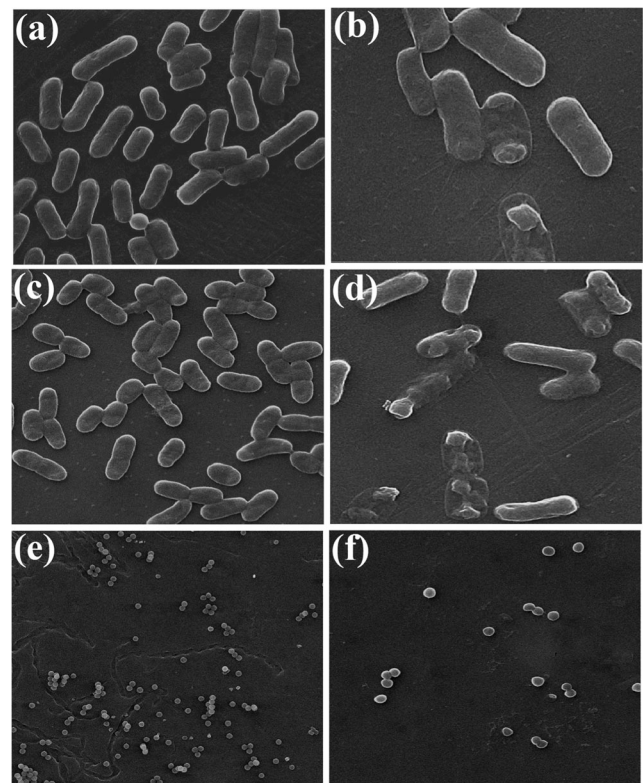
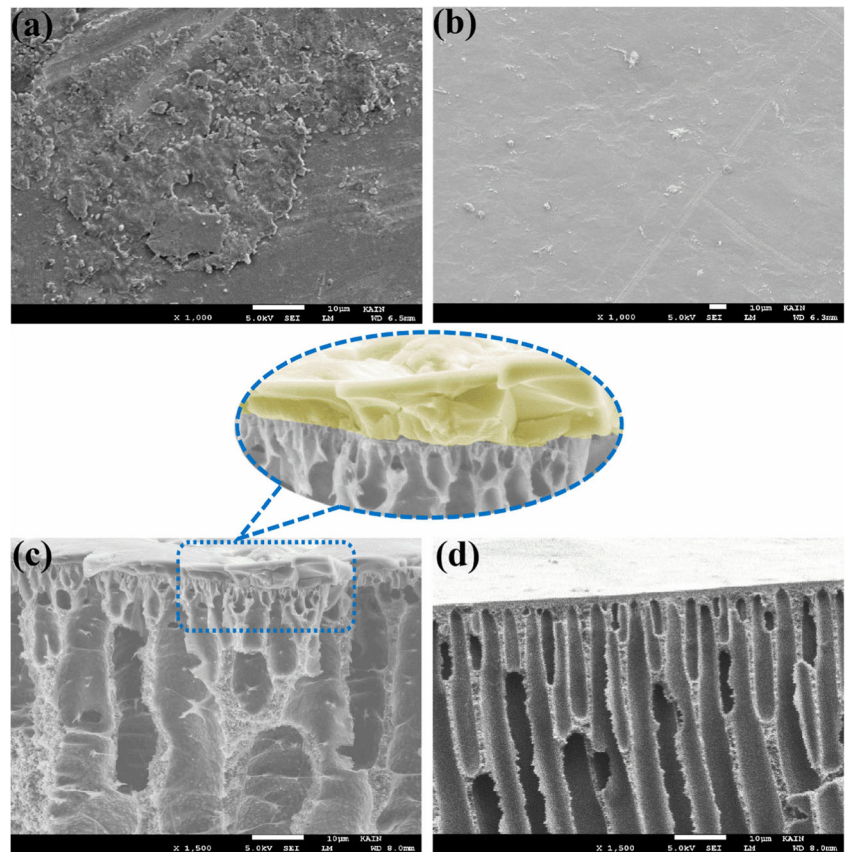


Fig. 4 SEM micrograph showing adhesion tests: Morphology of *E. coli* (**a**, **b**), *P. aeruginosa* (**c**, **d**), and *S. aureus* (**e**, **f**) on pure PPSU membrane (images: **a**, **c**, and **e**) and PPSU/COOH-GO nanocomposite membrane (images: **b**, **d**, and **f**)

Fig. 5 The membranes morphology after antifouling study using a BSA fouling agent: **a–c** surface and cross section of pure PPSU, **c** the dotted boxes for deposit foulants layer on the surface of membrane, and **b–d** surface and cross section of PPSU/COOH-GO nanocomposite membrane



S. aureus on PPSU membranes covered a larger surface area and had a smooth and intact appearance, indicating that the cells were normal and healthy (Fig. 4a, c, e). The biofilm formed on PPSU/COOH-GO nanocomposite membranes displayed an altered morphology and was scattered over the membrane surface as individual cells rather than as the visual appearance that is typical of a biofilm (Fig. 4b, d, f). Scanning electron micrographs revealed that the PPSU/COOH-GO nanocomposite membrane inhibited attachment, colonization, and biofilm formation by the three tested bacteria (Fig. 4b, d, and f). Furthermore, an obvious increase in size, roughness, indentations, and elongation of *E. coli* and *P. aeruginosa* cells suggested that the cell wall and membrane of the Gram-negative bacteria were severely damaged due to direct contact with the PPSU/COOH-GO nanocomposite membrane (Fig. 4b, d). The exact mode of action of the GO-based polymeric membrane is not completely understood. (Liu et al. 2011) reported the irreversible damage and destruction of *E. coli* due the direct contact with of the graphene-based membrane surface. Oxidative stress and lipid peroxidation have been proposed to play major roles in the killing of bacterial cells when exposed to the GO-based polymeric membrane (Liu et al. 2011; Gurunathan et al. 2012; Krishnamoorthy et al. 2012). The sharp edges of graphene may penetrate the bacteria and disrupting their membrane integrity (Akhavan and Ghaderi 2010; Hu et al. 2010). In the current study, the effect

of COOH-GO on bacterial adhesion was more pronounced for the two Gram-negative bacteria than for *S. aureus*. The reduced adhesion of *S. aureus* could be attributed due to the thick peptidoglycan layer. Our collective data demonstrating the strong antimicrobial and antiadhesion properties of the PPSU/COOH-GO nanocomposite membrane agreed with the excellent performance reported for other types of GO-coated membranes, such as polyethersulfone, polypropylene, polyvinylidene fluoride, polyamide, and polysulfone (Perreault et al. 2013; Yu et al. 2013b; He et al. 2015; Zhang et al. 2015; Zeng et al. 2016).

Antifouling properties of the nanocomposite membrane

The antifouling properties of a membrane can be ascribed to several mechanisms, which include the foulants that are adsorbed or deposited into or on the membrane, cake layer formation on the membrane surface, and morphological and physical changes during the prolonged use of the membrane for filtration. PPSU/COOH-GO nanocomposite membrane incorporating the COOH-GO nanomaterial effectively improved the membrane antifouling properties, as it was shown in surface and cross-section morphology (Fig. 5). We performed a long-term filtration experiment using BSA to explore the antifouling properties. The flux recovery ratio

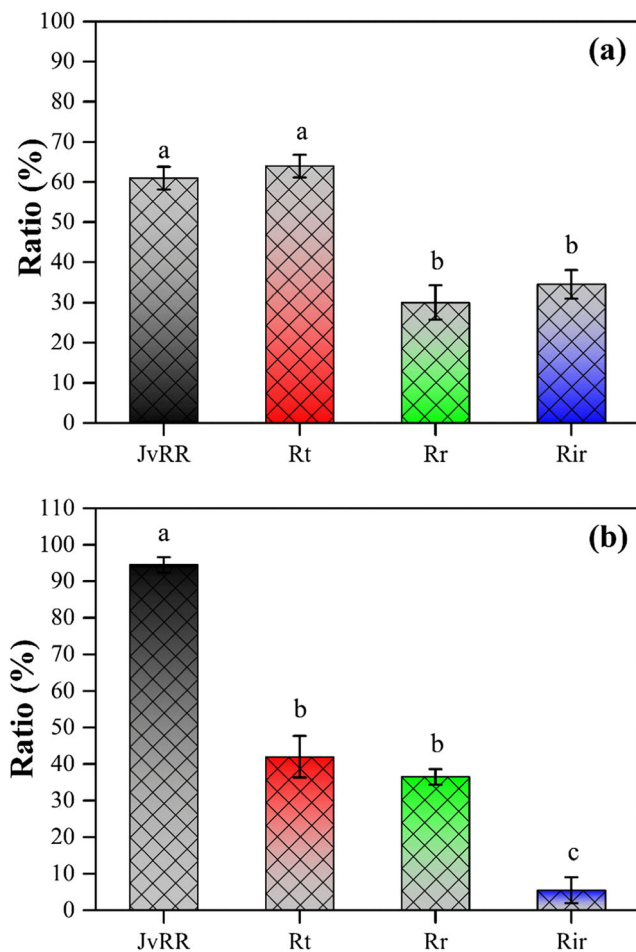


Fig. 6 Antifouling properties study: the variation of fouling parameters of **a** pure PPSU and **b** PPSU/COOH-GO nanocomposite membranes at the BSA protein experiment. Different letters indicate significant differences ($p < 0.05$) between treatments using a one-way ANOVA with a post-hoc Tukey's HSD test

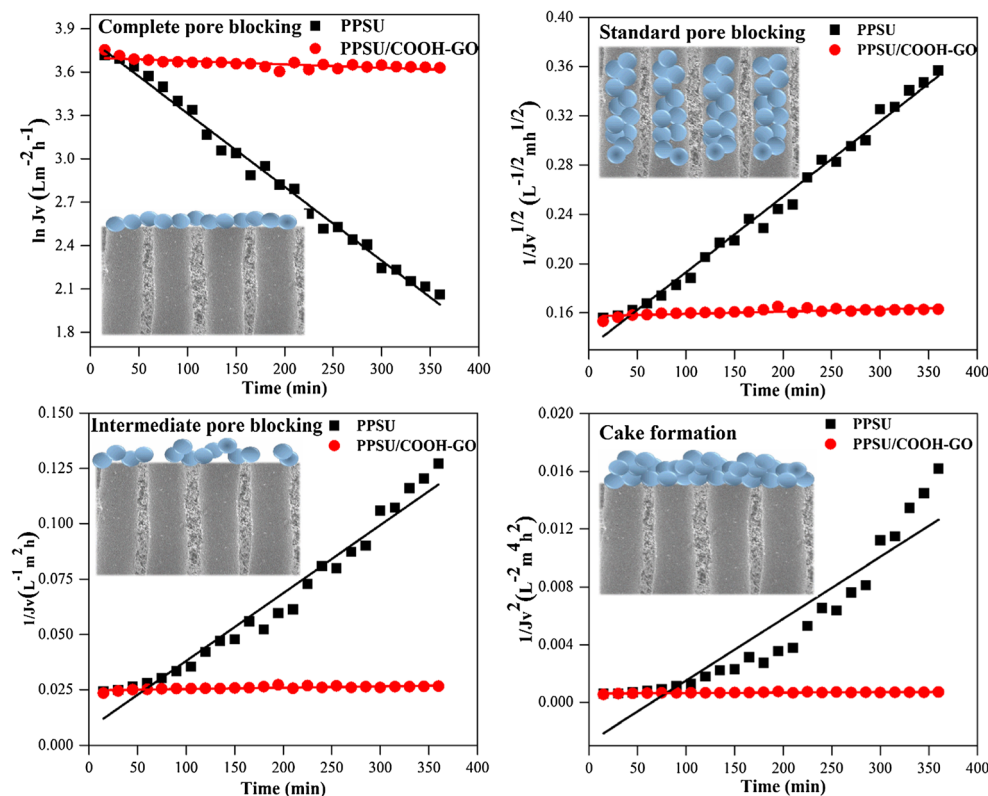
(J_vRR) was evaluated, and the results are shown in Fig. 6. The PPSU/COOH-GO nanocomposite membrane displayed a higher J_vRR value of 95.3% than the pure PPSU membrane (61.7%) as shown in Fig. 6a, b. The outstanding antifouling property of the nanocomposite membrane was attributed to the nanoparticles embedded in the PPSU matrix. The markedly higher J_vRR value indicated that the deposition of the BSA on the membrane surface could be directly prevented by hydraulic cleaning owing to the surface charge and surface hydrophilicity of the nanocomposite membrane. The excellent antifouling properties of the PPSU/COOH-GO nanocomposite membrane reflected the presence of numerous carboxylic groups of the GO nanoparticles on the membrane surface. The carboxylic groups increased the negative charge of the membrane and enhanced its hydrophilicity (Shukla et al. 2018). The negative charge and hydrophilicity of the surface effectively decreased the fouling via the adsorption of water molecules and the subsequent increase in the electrostatic

repulsion between the surfaces of membrane and protein, which hindered cake formation and adsorption of foulants onto the membrane surface also shown the model in Fig. 1 (Mo et al. 2012; Kaleekkal et al. 2016). To investigate the antifouling properties of the prepared membranes in more detail, during BSA filtration, R_t , R_r , and R_{ir} were determined. As revealed in Fig. 6a, R_t and R_{ir} for the pure PPSU membrane were 64.0% and 34.5%, respectively. These ratios were less for the nanocomposite membrane (42% and 5.5%, respectively). The reduced R_t of the PPSU/COOH-GO nanocomposite membrane was indicative of the reduced deposition of foulants and reduced adsorption to the membrane surface. These reductions would contribute to a very low flux decline. On the other hand, the R_{ir} values indicate that the foulants could not be removed by physical cleaning due to the strong attachment of foulants molecules to the surface or their plugging of the membrane pores. The R_r of the PPSU and nanocomposite membranes (30% and 36.5%, respectively) indicated that the foulant molecules were easily eliminated by simple backwashing through hydraulic cleaning and recovery of water flux for loose deposition of the cake layer on the PPSU/COOH-GO nanocomposite membrane surface. The F , df , and P values were showed for pure PPSU membrane 53.315, 3, and 0.001 and for PPSU/COOH-GO nanocomposite membrane 203.922, 3, and 0.000 against the protein fouling. For comparison, pure PPSU membrane and PPSU/COOH-GO nanocomposite membrane incorporating the COOH-GO nanomaterial and their antifouling properties were compared by using through the statistical analysis. Foregoing explanations support the idea that, for the nanocomposite membrane, adhesion forces, such as Van der Waals force, electrostatic force, hydrogen bonding force, and hydrophilic force, are responsible for the elimination of the BSA foulant at the membrane surface because the surface of membrane harbors many carboxylic functional groups and provides good clamping of the membranes (Ayyaru and Ahn 2017; Chen et al. 2018). The above results markedly demonstrate the superior antifouling character of PPSU/COOH-GO nanocomposite membrane.

Fouling mechanisms

Continuing the evaluation, Hermia's models were applied to understand the fouling mechanisms occurring throughout membrane filtration with BSA. The experimental fouling data were fit with the models to predict the flux decline of pure PPSU and nanocomposite PPSU/COOH-GO membranes (Fig. 7). The correlation coefficients (R^2) were used to assess the fitted model parameters and identify the type of pore blockings. The findings are summarized in Table 1. The R^2 values that were obtained were the highest, indicating the suitability of the theoretical Hermia models to describe membrane fouling (Ng et al. 2014). The obtained experimental and model-predicted data provided an indication of the

Fig. 7 Obtained volumetric flux during filtration of BSA solution; experimental data and Hermia fouling models of the fabricated pure PPSU and PPSU/COOH-GO nanocomposite membranes



predominant factor of the gradual temporal decline of the flux. The cake formation model was the dominant mechanism for a sample containing COOH-GO nanomaterials (Fig. 7). Thus, cake formation was implicated as the primary fouling mechanism, followed by intermediate pore blocking. For pure PPSU membranes, the best modeling of the data occurred with the complete blocking mechanism. Data from the combined fouling models as well as experimental data for the membranes are depicted in Fig. 7. Hermia's models displayed a lack of fit for the experimental flux decline data over the entire time interval for PPSU membranes and indicated the involvement of membrane fouling in several simultaneous mechanisms (Torkamanzadeh et al. 2016). The findings can be interesting as indicating that the fouling of PPSU membranes very likely is due to the membrane's lower surface charge and hydrophobic characteristic. The BSA flux of the membranes depended on the membrane hydrophilicity as well as pore structure. The results of the combined fouling mechanisms confirm the

positive influence of the embedded COOH-GO in the membrane surface in the resistance to membrane fouling.

Conclusions

To develop a cost-effective membrane technology for the bio-fouling, such as that caused by microorganisms or protein in an aqueous environment, the antimicrobial and antifouling properties of a PPSU/COOH-GO nanocomposite membrane fabricated through an immersion precipitation phase inversion process were evaluated. The nanocomposite had excellent antibacterial properties, with higher bacteriostasis rate for two Gram-negative bacteria (74.2% for *E. coli* and 81.1% for *P. aeruginosa*) compared to the 41.9% rate for the Gram-positive bacterium *S. aureus*. *E. coli* and *P. aeruginosa* were more susceptible than *S. aureus*. In addition, the nanocomposite membrane inhibited attachment, colonization, and biofilm formation by these bacteria. The cell wall and outer membrane of *E. coli* and *P. aeruginosa* were susceptible to physical damage upon direct contact with the PPSU/COOH-GO nanocomposite membrane. Furthermore, the surface of the nanocomposite membrane significantly enhanced antifouling, as demonstrated by a less irreversible fouling and higher flux recovery ratio. The cake formation and complete blocking were the main fouling mechanisms for the membranes. Hence, the prepared PPSU/COOH-GO nanocomposite membrane

Table 1 Obtained correlation coefficient (R^2) values based on Hermia fouling models during membrane fouling

Blocking models	PPSU	PPSU/COOH-GO
Complete pore blocking ($n = 2$)	0.9911	0.5774
Standard blocking ($n = 1.5$)	0.9882	0.5786
Intermediate blocking ($n = 1$)	0.9622	0.5794
Cake formation ($n = 0$)	0.8665	0.5802

demonstrated excellent antimicrobial and antifouling properties when tested against biofoulant; thus, the developed GO-based nanocomposite membrane is an optimum choice for water treatment.

Acknowledgments The authors thank the Deanship of Scientific Research and RSSU at King Saud University for their technical support.

Funding information The authors extend their appreciation to the Deanship of Scientific Research at King Saud University for funding this work through research group no (RG-1439-85).

Abbreviations PPSU, polyphenylsulfone; COOH-GO, carboxyl-functionalized graphene oxide; *E. coli*, *Escherichia coli*; *P. aeruginosa*, *Pseudomonas aeruginosa*; *S. aureus*, *Staphylococcus aureus*; BSA, bovine serum albumin; CFU, colony-forming unit; TMP, transmembrane pressure; J_w , pure water volumetric flux; J_{vp} , foulant volumetric flux; J_{v1} , final water volumetric flux; J_{vRR} , flux recovery ratio; R_t , total fouling ratio; R_r , reversible fouling ratio; R_{ir} , irreversible fouling ratio; J_{vp0} , initial volume flow rate; J_{vpt} , volume flow at a particular time; K_c , membrane surface area blocked per unit of permeate volume; t , time; K_{ss} , constant of the standard blocking model; K_i , constant of the intermediate blocking model; K_{cf} , constant of the cake formation model

References

- Abdel-Karim A, Leaper S, Alberto M, Vijayaraghavan A, Fan X, Holmes SM, Souaya ER, Badawy MI, Gorgojo P (2018) High flux and fouling resistant flat sheet polyethersulfone membranes incorporated with graphene oxide for ultrafiltration applications. *Chem Eng J* 334:789–799. <https://doi.org/10.1016/j.cej.2017.10.069>
- Abinaya M, Vaseeharan B, Divya M, Vijayakumar S, Govindarajan M, Alharbi NS, Khaled JM, al-anbr MN, Benelli G (2018) Structural characterization of *Bacillus licheniformis* Dabhl exopolysaccharide—antimicrobial potential and larvicidal activity on malaria and Zika virus mosquito vectors. *Environ Sci Pollut Res* 25:18604–18619. <https://doi.org/10.1007/s11356-018-2002-6>
- Ahmed F, Santos CM, Vergara RAMV, Tria MCR, Advincula R, Rodrigues DF (2012) Antimicrobial applications of electroactive PVK-SWNT nanocomposites. *Environ Sci Technol* 46:1804–1810. <https://doi.org/10.1021/es202374e>
- Akhavan O, Ghaderi E (2010) Toxicity of graphene and graphene oxide nanowalls against bacteria. *ACS Nano* 4:5731–5736. <https://doi.org/10.1021/nn101390x>
- Ansari MA, Khan HM, Khan AA, Ahmad MK, Mahdi AA, Pal R, Cameotra SS (2014) Interaction of silver nanoparticles with *Escherichia coli* and their cell envelope biomolecules. *J Basic Microbiol* 54:905–915. <https://doi.org/10.1002/jobm.201300457>
- Ayyaru S, Ahn YH (2017) Application of sulfonic acid group functionalized graphene oxide to improve hydrophilicity, permeability, and antifouling of PVDF nanocomposite ultrafiltration membranes. *J Memb Sci* 525:210–219. <https://doi.org/10.1016/j.memsci.2016.10.048>
- Benelli G (2018) Plant-borne compounds and nanoparticles: challenges for medicine, parasitology and entomology. *Environ Sci Pollut Res* 25:10149–10150. <https://doi.org/10.1007/s11356-017-9960-y>
- Ben-Sasson M, Zodrow KR, Genggeng Q, Kang Y, Giannelis EP, Elimelech M (2014) Surface functionalization of thin-film composite membranes with copper nanoparticles for antimicrobial surface properties. *Environ Sci Technol* 48:384–393. <https://doi.org/10.1021/es404232s>
- Bogdanović U, Vodnik V, Mitrić M, Dimitrijević S, Škapin SD, Žunić V, Budimir M, Stoiljković M (2015) Nanomaterial with high antimicrobial efficacy copper/polyaniline nanocomposite. *ACS Appl Mater Interfaces* 7:1955–1966. <https://doi.org/10.1021/am507746m>
- Chen F, Shi X, Chen X, Chen W (2018) Preparation and characterization of amphiphilic copolymer PVDF-g-PMABS and its application in improving hydrophilicity and protein fouling resistance of PVDF membrane. *Appl Surf Sci* 427:787–797. <https://doi.org/10.1016/j.apsusc.2017.08.096>
- Chung YT, Mahmoudi E, Mohammad AW, Benamor A, Johnson D, Hilal N (2017) Development of polysulfone-nanohybrid membranes using ZnO-GO composite for enhanced antifouling and antibacterial control. *Desalination* 402:123–132. <https://doi.org/10.1016/j.desal.2016.09.030>
- Corbatón-Báguena M-J, Álvarez-Blanco S, Vincent-Vela M-C (2018) Evaluation of fouling resistances during the ultrafiltration of whey model solutions. *J Clean Prod* 172:358–367. <https://doi.org/10.1016/j.jclepro.2017.10.149>
- Emadzadeh D, Ghanbari M, Lau WJ, Rahbari-Sisakht M, Rana D, Matsuura T, Kruczek B, Ismail AF (2017) Surface modification of thin film composite membrane by nanoporous titanate nanoparticles for improving combined organic and inorganic antifouling properties. *Mater Sci Eng C* 75:463–470. <https://doi.org/10.1016/j.msec.2017.02.079>
- Eng AYS, Sofer Z, Sedmidubský D, Pumera M (2017) Synthesis of carboxylated-graphenes by the Kolbe-Schmitt process. *ACS Nano* 11:1789–1797. <https://doi.org/10.1021/acsnano.6b07746>
- Gao Q, Yu M, Su Y, Xie M, Zhao X, Li P, Ma PX (2017a) Rationally designed dual functional block copolymers for bottlebrush-like coatings: in vitro and in vivo antimicrobial, antibiofilm, and antifouling properties. *Acta Biomater* 51:112–124. <https://doi.org/10.1016/j.actbio.2017.01.061>
- Gao Y, Wu J, Ren X, Tan X, Hayat T, Alsaedi A, Cheng C, Chen C (2017b) Impact of graphene oxide on the antibacterial activity of antibiotics against bacteria. *Environ Sci Nano* 4:1016–1024. <https://doi.org/10.1039/C7EN00052A>
- Gurunathan S, Han JW, Dayem AA et al (2012) Oxidative stress-mediated antibacterial activity of graphene oxide and reduced graphene oxide in *Pseudomonas aeruginosa*. *Int J Nanomedicine* 7:5901–5914. <https://doi.org/10.2147/IJN.S37397>
- He L, Dumée LF, Feng C, Velleman L, Reis R, She F, Gao W, Kong L (2015) Promoted water transport across graphene oxide–poly(amide) thin film composite membranes and their antibacterial activity. *Desalination* 365:126–135. <https://doi.org/10.1016/j.desal.2015.02.032>
- Ho KC, Teow YH, Ang WL, Mohammad AW (2017) Novel GO/OMWCNTs mixed-matrix membrane with enhanced antifouling property for palm oil mill effluent treatment. *Sep Purif Technol* 177:337–349. <https://doi.org/10.1016/j.seppur.2017.01.014>
- Hou S, Xing J, Dong X, Zheng J, Li S (2017) Integrated antimicrobial and antifouling ultrafiltration membrane by surface grafting PEO and N-chloramine functional groups. *J Colloid Interface Sci* 500:333–340. <https://doi.org/10.1016/j.jcis.2017.04.028>
- Hu W, Peng C, Luo W, Lv M, Li X, Li D, Huang Q, Fan C (2010) Graphene-based antibacterial paper. *ACS Nano* 4:4317–4323. <https://doi.org/10.1021/nn101097v>
- Hu M, Zheng S, Mi B (2016) Organic fouling of graphene oxide membranes and its implications for membrane fouling control in engineered osmosis. *Environ Sci Technol* 50:685–693. <https://doi.org/10.1021/acs.est.5b03916>
- Hu Y, Lü Z, Wei C, Yu S, Liu M, Gao C (2018) Separation and antifouling properties of hydrolyzed PAN hybrid membranes prepared via in-situ sol-gel SiO₂nanoparticles growth. *J Membr Sci* 545:250–258. <https://doi.org/10.1016/j.memsci.2017.09.081>
- Huang H, Yu J, Guo H, Shen Y, Yang F, Wang H, Liu R, Liu Y (2018) Improved antifouling performance of ultrafiltration membrane via

- preparing novel zwitterionic polyimide. *Appl Surf Sci* 427:38–47. <https://doi.org/10.1016/j.apsusc.2017.08.004>
- Ji H, Sun H, Qu X (2016) Antibacterial applications of graphene-based nanomaterials: recent achievements and challenges. *Adv Drug Deliv Rev* 105:176–189. <https://doi.org/10.1016/j.addr.2016.04.009>
- Kaleekkal NJ, Thanigaivelan A, Rana D, Mohan D (2016) Studies on carboxylated graphene oxide incorporated polyetherimide mixed matrix ultrafiltration membranes. *Mater Chem Phys* 186:146–158. <https://doi.org/10.1016/j.matchemphys.2016.10.040>
- Koh E, Lee YT (2017) Antimicrobial activity and fouling resistance of a polyvinylidene fluoride (PVDF) hollow-fiber membrane. *J Ind Eng Chem* 47:260–271. <https://doi.org/10.1016/j.jiec.2016.11.042>
- Krishnamoorthy K, Veerapandian M, Zhang LH, Yun K, Kim SJ (2012) Antibacterial efficiency of graphene nanosheets against pathogenic bacteria via lipid peroxidation. *J Phys Chem C* 116:17280–17287. <https://doi.org/10.1021/jp3047054>
- Lee A, Elam JW, Darling SB (2016) Membrane materials for water purification: design, development, and application. *Environ Sci Water Res Technol* 2:17–42. <https://doi.org/10.1039/C5EW00159E>
- Liu S, Zeng TH, Hoffmann M, Burcombe E, Wei J, Jiang R, Kong J, Chen Y (2011) Antibacterial activity of graphite, graphite oxide, graphene oxide, and reduced graphene oxide: membrane and oxidative stress. *ACS Nano* 5:6971–6980. <https://doi.org/10.1021/nn202451x>
- Liu C, Faria AF, Ma J, Elimelech M (2017) Mitigation of biofilm development on thin-film composite membranes functionalized with Zwitterionic polymers and silver nanoparticles. *Environ Sci Technol* 51:182–191. <https://doi.org/10.1021/acs.est.6b03795>
- Lu X, Feng X, Werber JR, Chu C, Zucker I, Kim JH, Osuji CO, Elimelech M (2017) Enhanced antibacterial activity through the controlled alignment of graphene oxide nanosheets. *Proc Natl Acad Sci* 114: E9793–E9801. <https://doi.org/10.1073/pnas.1710996114>
- Luyts K, Napierska D, Nemery B, Hoet PHM (2013) How physico-chemical characteristics of nanoparticles cause their toxicity: complex and unresolved interrelations. *Environ Sci Impacts* 15:23–38. <https://doi.org/10.1039/c2em30237c>
- Ma R, Ji YL, Guo YS, Mi YF, An QF, Gao CJ (2017) Fabrication of antifouling reverse osmosis membranes by incorporating zwitterionic colloids nanoparticles for brackish water desalination. *Desalination* 416:35–44. <https://doi.org/10.1016/j.desal.2017.04.016>
- Mejías Carpio IE, Santos CM, Wei X, Rodrigues DF (2012) Toxicity of a polymer–graphene oxide composite against bacterial planktonic cells, biofilms, and mammalian cells. *Nanoscale* 4:4746–4756. <https://doi.org/10.1039/c2nr30774j>
- Mo Y, Tiraferri A, Yip NY, Adout A, Huang X, Elimelech M (2012) Improved antifouling properties of polyamide nanofiltration membranes by reducing the density of surface carboxyl groups. *Environ Sci Technol* 46:13253–13261. <https://doi.org/10.1021/es303673p>
- Moradi G, Zinadini S, Rajabi L, Dadari S (2018) Fabrication of high flux and antifouling mixed matrix fumarate-alumoxane/PAN membranes via electrospinning for application in membrane bioreactors. *Appl Surf Sci* 427:830–842. <https://doi.org/10.1016/j.apsusc.2017.09.039>
- Morelos-Gomez A, Cruz-Silva R, Muramatsu H, Ortiz-Medina J, Araki T, Fukuyo T, Tejima S, Takeuchi K, Hayashi T, Terrones M, Endo M (2017) Effective NaCl and dye rejection of hybrid graphene oxide/graphene layered membranes. *Nat Nanotechnol* 12:1083–1088. <https://doi.org/10.1038/nnano.2017.160>
- Nasrollahi N, Vatanpour V, Aber S, Mahmoodi NM (2018) Preparation and characterization of a novel polyethersulfone (PES) ultrafiltration membrane modified with a CuO/ZnO nanocomposite to improve permeability and antifouling properties. *Sep Purif Technol* 192: 369–382. <https://doi.org/10.1016/j.seppur.2017.10.034>
- Ng CY, Mohammad AW, Ng LY, Jahim JM (2014) Membrane fouling mechanisms during ultrafiltration of skimmed coconut milk. *J Food Eng* 142:190–200. <https://doi.org/10.1016/j.jfoodeng.2014.06.005>
- Perreault F, Tousley ME, Elimelech M (2013) Thin-film composite polyamide membranes functionalized with biocidal graphene oxide nanosheets. *Environ Sci Technol Lett* 1:71–76. <https://doi.org/10.1021/ez4001356>
- Perreault F, Fonseca de Faria A, Elimelech M (2015) Environmental applications of graphene-based nanomaterials. *Chem Soc Rev* 44: 5861–5896. <https://doi.org/10.1039/C5CS00021A>
- Perreault F, Jaramillo H, Xie M, Ude M, Nghiem LD, Elimelech M (2016) Biofouling mitigation in forward osmosis using graphene oxide functionalized thin-film composite membranes. *Environ Sci Technol* 50:5840–5848. <https://doi.org/10.1021/acs.est.5b06364>
- Qiu WZ, Zhao ZS, Du Y et al (2017) Antimicrobial membrane surfaces via efficient polyethyleneimine immobilization and cationization. *Appl Surf Sci* 426:972–979. <https://doi.org/10.1016/j.apsusc.2017.07.217>
- Safarpour M, Vatanpour V, Khataee A (2016) Preparation and characterization of graphene oxide/TiO₂ blended PES nanofiltration membrane with improved antifouling and separation performance. *Desalination* 393:65–78. <https://doi.org/10.1016/j.desal.2015.07.003>
- Sanchez VC, Jachak A, Hurt RH, Kane AB (2012) Biological interactions of graphene-family nanomaterials: an interdisciplinary review. *Chem Res Toxicol* 25:15–34. <https://doi.org/10.1021/tx200339h>
- Sawada I, Fachrul R, Ito T, Ohmukai Y, Maruyama T, Matsuyama H (2012) Development of a hydrophilic polymer membrane containing silver nanoparticles with both organic antifouling and antibacterial properties. *J Membr Sci* 387–388:1–6. <https://doi.org/10.1016/j.memsci.2011.06.020>
- Shanmuganathan R, MubarakAli D, Prabakar D, Muthukumar H, Thajuddin N, Kumar SS, Pugazhendhi A (2018) An enhancement of antimicrobial efficacy of biogenic and ceftriaxone-conjugated silver nanoparticles: green approach. *Environ Sci Pollut Res* 25: 10362–10370. <https://doi.org/10.1007/s11356-017-9367-9>
- Shannon MA, Bohn PW, Elimelech M, Georgiadis JG, Mariñas BJ, Mayes AM (2008) Science and technology for water purification in the coming decades. *Nature* 452:301–310. <https://doi.org/10.1038/nature06599>
- Shockravi A, Vatanpour V, Najjar Z, Bahadori S, Javadi A (2017) A new high performance polyamide as an effective additive for modification of antifouling properties and morphology of asymmetric PES blend ultrafiltration membranes. *Microporous Mesoporous Mater* 246:24–36. <https://doi.org/10.1016/j.micromeso.2017.03.013>
- Shukla AK, Alam J, Alhoshan M, Dass LA, Muthumareeswaran MR (2017) Development of a nanocomposite ultrafiltration membrane based on polyphenylsulfone blended with graphene oxide. *Sci Rep* 7:41976–41987. <https://doi.org/10.1038/srep41976>
- Shukla AK, Alam J, Alhoshan M, Arockiasamy Dass L, Ali FAA, M. R M, Mishra U, Ansari MA (2018) Removal of heavy metal ions using a carboxylated graphene oxide-incorporated polyphenylsulfone nanofiltration membrane. *Environ Sci Water Res Technol* 4:438–448. <https://doi.org/10.1039/C7EW00506G>
- Srinivasan R, Vigneshwari L, Rajavel T, Durgadevi R, Kannappan A, Balamurugan K, Pandima Devi K, Veera Ravi A (2018) Biogenic synthesis of silver nanoparticles using *Piper betle* aqueous extract and evaluation of its anti-quorum sensing and antibiofilm potential against uropathogens with cytotoxic effects: an in vitro and in vivo approach. *Environ Sci Pollut Res* 25:10538–10554. <https://doi.org/10.1007/s11356-017-1049-0>
- Torkamanzadeh M, Jahanshahi M, Peyravi M, Rad AS (2016) Comparative experimental study on fouling mechanisms in nanoporous membrane: cheese whey ultrafiltration as a case study. *Water Sci Technol* 74:2737–2750. <https://doi.org/10.2166/wst.2016.352>
- Wang YN, Tang CY (2011) Fouling of nanofiltration, reverse osmosis, and ultrafiltration membranes by protein mixtures: the role of inter-foulant-species interaction. *Environ Sci Technol* 45:6373–6379. <https://doi.org/10.1021/es2013177>

- Wang W, Zhu L, Shan B, Xie C, Liu C, Cui F, Li G (2018) Preparation and characterization of SLS-CNT/PES ultrafiltration membrane with antifouling and antibacterial properties. *J Membr Sci* 548: 459–469. <https://doi.org/10.1016/j.memsci.2017.11.046>
- Whitehead KA, Vaidya M, Liauw CM, Brownson DAC, Ramalingam P, Kamieniak J, Rowley-Neale SJ, Tetlow LA, Wilson-Nieuwenhuis JST, Brown D, McBain AJ, Kulandaivel J, Banks CE (2017) Antimicrobial activity of graphene oxide-metal hybrids. *Int Biodeterior Biodegrad* 123:182–190. <https://doi.org/10.1016/j.ibiod.2017.06.020>
- Xu Q, Zeng M, Feng Z, Yin D, Huang Y, Chen Y, Yan C, Li R, Gu Y (2016) Understanding the effects of carboxylated groups of functionalized graphene oxide on the curing behavior and intermolecular interactions of benzoxazine nanocomposites. *RSC Adv* 6:31484–31496. <https://doi.org/10.1039/C5RA28016H>
- Xu Z, Liao J, Tang H, Li N (2017) Antifouling polysulfone ultrafiltration membranes with pendent sulfonamide groups. *J Membr Sci* 548: 481–489. <https://doi.org/10.1016/j.memsci.2017.11.064>
- You X, Ma T, Su Y, Wu H, Wu M, Cai H, Sun G, Jiang Z (2017) Enhancing the permeation flux and antifouling performance of polyamide nanofiltration membrane by incorporation of PEG-POSS nanoparticles. *J Membr Sci* 540:454–463. <https://doi.org/10.1016/j.memsci.2017.06.084>
- Yousefi M, Dadashpour M, Hejazi M, Hasanzadeh M, Behnam B, de la Guardia M, Shadjou N, Mokhtarzadeh A (2017) Anti-bacterial activity of graphene oxide as a new weapon nanomaterial to combat multidrug-resistance bacteria. *Mater Sci Eng C* 74:568–581. <https://doi.org/10.1016/j.msec.2016.12.125>
- Yu H, Zhang X, Zhang Y, Liu J, Zhang H (2013a) Development of a hydrophilic PES ultrafiltration membrane containing SiO₂@N-Halamine nanoparticles with both organic antifouling and antibacterial properties. *Desalination* 326:69–76. <https://doi.org/10.1016/j.desal.2013.07.018>
- Yu L, Zhang Y, Zhang B, Liu J, Zhang H, Song C (2013b) Preparation and characterization of HPEI-GO/PES ultrafiltration membrane with antifouling and antibacterial properties. *J Membr Sci* 447: 452–462. <https://doi.org/10.1016/j.memsci.2013.07.042>
- Yu S, Liu J, Zhu W, Hu ZT, Lim TT, Yan X (2015) Facile room-temperature synthesis of carboxylated graphene oxide-copper sulfide nanocomposite with high photodegradation and disinfection activities under solar light irradiation. *Sci Rep* 5:16369–16380. <https://doi.org/10.1038/srep16369>
- Zeng Z, Yu D, He Z, Liu J, Xiao FX, Zhang Y, Wang R, Bhattacharyya D, Tan TTY (2016) Graphene oxide quantum dots covalently functionalized PVDF membrane with significantly-enhanced bactericidal and antibiofouling performances. *Sci Rep* 6:20142–20152. <https://doi.org/10.1038/srep20142>
- Zhang ZB, Wu JJ, Su Y, Zhou J, Gao Y, Yu HY, Gu JS (2015) Layer-by-layer assembly of graphene oxide on polypropylene macroporous membranes via click chemistry to improve antibacterial and antifouling performance. *Appl Surf Sci* 332:300–307. <https://doi.org/10.1016/j.apsusc.2015.01.193>
- Zhang DY, Hao Q, Liu J, Shi YS, Zhu J, Su L, Wang Y (2018a) Antifouling polyimide membrane with grafted silver nanoparticles and zwitterion. *Sep Purif Technol* 192:230–239. <https://doi.org/10.1016/j.seppur.2017.10.018>
- Zhang J, Xu Y, Chen S et al (2018b) Enhanced antifouling and antibacterial properties of poly (ether sulfone) membrane modified through blending with sulfonated poly (aryl ether sulfone) and copper nanoparticles. *Appl Surf Sci* 434:806–815. <https://doi.org/10.1016/j.apsusc.2017.11.007>
- Zhu L, Song H, Zhang D, Wang G, Zeng Z, Xue Q (2017) Negatively charged polysulfone membranes with hydrophilicity and antifouling properties based on in situ cross-linked polymerization. *J Colloid Interface Sci* 498:136–143. <https://doi.org/10.1016/j.jcis.2017.03.055>
- Zodrow K, Brunet L, Mahendra S, Li D, Zhang A, Li Q, Alvarez PJ (2009) Polysulfone ultrafiltration membranes impregnated with silver nanoparticles show improved biofouling resistance and virus removal. *Water Res* 43:715–723. <https://doi.org/10.1016/j.watres.2008.11.014>
- Zou F, Zhou H, Jeong DY, Kwon J, Eom SU, Park TJ, Hong SW, Lee J (2017) Wrinkled surface-mediated antibacterial activity of graphene oxide nanosheets. *ACS Appl Mater Interfaces* 9:1343–1351. <https://doi.org/10.1021/acsami.6b15085>